DIAGNOSTYKA, 2017, Vol. 18, No. 1

ISSN 1641-6414
e-ISSN 2449-5220

FOUR MODELS OF TRIBOLOGICAL WEAR OF TURBINE JET ENGINE BEARINGS BASED ON METHODS OF ELECTRICAL GENERATOR SIGNAL ANALYSIS

Andrzej GĘBURA
Air Force Institute of Technology, 01-494, Warszawa 46, Księcia Bolesława 6
e-mail:andrzej.gebura@itwl.pl

Summary

The article describes test results of rolling bearings conducted on turbojets, with the simultaneous use of two diagnostics methods: FAM-C and FDM-A [7]. For these methods, no installation of additional sensors on the aircraft is needed – the on-board electric generators are used as sensors. The „FAM-C" method uses the aircraft's alternating current (AC) tachometer generator, whereas the "FDM-A" method uses the direct current (DC) commutator-type generator. Spectrum of angular velocity of individual bearings manifests itself in high frequency ranges (60-240 Hz for the tachometer generator, 3-10 kHz for the DC generator), making the oscillation signal resistant to noise. This frequency modulated signal can be picked up by measuring instruments in any point of the aircraft electrical system. After detection the initial signal is obtained. Measurement analysis can be easily automated [10]. During detection, the carrier frequency is filtered off. Currently, with the simultaneous use of correlated FAM-C and FDM-A methods, four models of rolling bearings wear can be detected: increase of aggregate friction, seizure of rolling elements, increase of radial clearances, increase of axial clearance. This division was made on the basis of observing the technical condition of rolling bearings on many (around 30) turbojets during its normal operation.

Key word: frequency analysis, DC generator, AC generator, bearing wear, increase of radial clearances, increase of axial clearances

CZTERY MODELE ZUŻYCIA TRIBOLOFICZNEGO PODPÓR ŁOŻYSKOWYCH W OPARCIU O ANALIZĘ SYGNAŁU PRĄDNICY

Streszczenie

Artykuł omawia wyniki badań łożysk tocznych przeprowadzonych na silnikach turboodrzutowych z jednoczesnym wykorzystaniem dwóch metod diagnostycznych: FAM-C i FDM-A [7]. W metodach tych nie trzeba instalować żadnych dodatkowych czujników - jako przetworniki wykorzystywane są prądnice pokładowe. W metodzie "FAM-C" wykorzystuje się prądnicę tachometryczną prądu przemiennego (AC), podczas gdy "FDM-A" wykorzystuje komutatorową prądnicę prądu stałego (DC). Widmo prędkości kątowej poszczególnych łożysk przenoszone jest przez prądnicę w pasmo wysokich zakresów częstotliwości (60-240 Hz dla prądnicy tachometrycznej, 3-10 kHz do prądnicy prądu stałego), dzięki czemu staje się bardzo odporne na zakłócenia. Ten modulowany częstotliwościowo sygnał może być odbierany przez przyrządy pomiarowe w każdym punkcie instalacji elektrycznej samolotu. Po detekcji odzyskiwany jest sygnał pierwotny. Analiza wyników z takiego pomiaru może być łatwo zautomatyzowana [10]. Podczas detekcji odfiltrowywana jest częstotliwość nośna. Przy jednoczesnym stosowaniu skorelowanych metod FAM-C i FDM-A, mogą być wykrywane cztery modele zużycia łożysk tocznych: zwiększonych oporów biernych, zaciśniętych elementów tocznych, zwiększanych luzów promieniowych, zwiększonych luzów osiowych. Podział ten został dokonany na bazie obserwacji stanu technicznego łożysk tocznych wielu (około 30-tu)egzemplarzy silników turboodrzutowych w czasie ich normalnej eksploatacji.

Słowa kluczowe: modulacja częstotliwości, prądnica prądu stałego, prądnica prądu przemiennego, zwiększone luzy promieniowe, zwiększone luzy podłużne.

1. INTRODUCTION

High rotational speeds in aircraft engines induce a significant load on mechanical joints – bearing elements in particular. Rolling element bearings that handle the increased speeds tend however to generate additional vibration which makes diagnostics and lubrication even more difficult. The an approach to monitoring bearing elements that utilizes the on-board electric generators (three phase tachogenerator and direct current commutator generator) as diagnostic sensors was suggested [11]. Nowadays, operation according to technical condition is getting more prevalent and fixed-interval overhauls of flight hours are more rarely used [21-23]. The operation according to technical condition requires reliable diagnostic

methods to detect onset and intensification of subassemblies' defect. Complicated aircraft assemblies and systems such as engines pose significant problems when it comes to identification, localization as well as prognosis of damage [23]. The FAM-C and FDM-A methods enable a non-invasive monitoring of multiple aircraft system elements simultaneously [11].

2. METHOD DESCRIPTION - ELECTRICAL GENERATOR AS A SENSOR

The FAM-C and FDM-A methods are, in essence, frequency analysis methods of mechanical systems, and are related to tip timing (TTM) and time of arrival (TOA) methods [3, 19]. In all of these methods there were applied the properties of frequency deviation $\Delta\omega$ $\{\Delta\omega_1, \Delta\omega_2, \Delta\omega_3 \ldots \Delta\omega_k\}$ resulting form mechanical defects of certain kinematic pairs, of which each one of them has the assigned rated speed forming subcarrier frequency $\{\omega_{N1}, \omega_{N2}, \omega_{N3} \ldots \omega_{Nk}\}$ – Fig. 1. However, the aforementioned methods differ from the others in this way that they do not require installation of any additional specialized monitoring sensors, as the on-board generators are used for this purpose. Thus, they build up a peculiar element of turbojet engine under consideration – in generator-converter similarly as in eye lens it is possible to read out the disturbances in the functioning of engine subassemblies. In the FAM-C method, the AC generator signal is analyzed, whereas in the FDM-A the DC generator signal is analyzed. Poles of the generators serve as local reluctance sensors located uniformly in phase space [11, 17] – Fig 2.

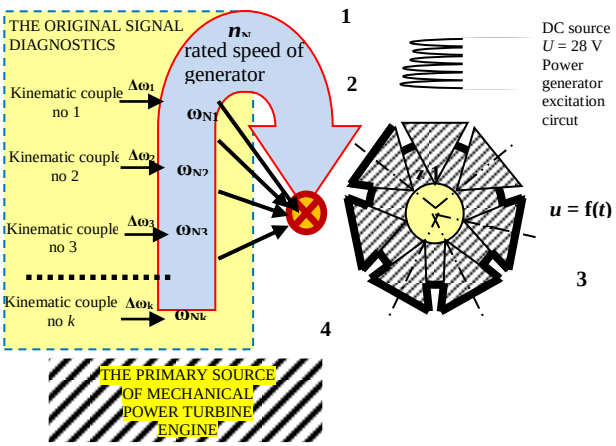

Fig. 1. Converter-generator as part of a peculiar monitoring mechanical driver unit: 1. – field winding of the generator stator, 2. – pole stator generator, 3. – rotor winding of the generator, 4. – rotor of generator

The generator produces a quasi-sinusoidal waveform:

$$u = f(t) = k\,B\,\sin(\omega_1\,t\,p) \tag{1}$$

where: p – number of pole pairs of generator stator, ω_1 [obr/min] – instantaneous value of generator angular speed, B [T] – magnetic induction in the crevice between the rotor and stator pole (N, S) – Fig. 2.

The transfer of normal line to the plane of rotor winding through the neutral magnetic line is a zero value of output voltage waveform. The transfer of this line below the centre of stator pole is a voltage extreme value. In this way, the quasi-sinusoidal waveform is generated – Fig 3.

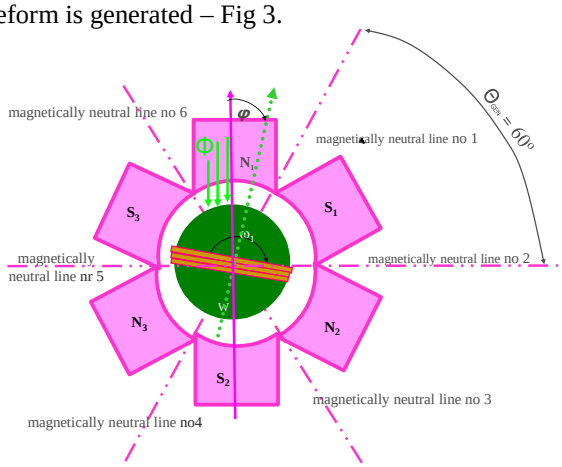

Fig. 2. Alternate current generators with three pairs of poles: N_1, N_2, N_3, S_1, S_2, S_3 – the magnetic poles of the stator of the generator, φ – momentary angular position of the rotor of the generator, Φ – the magnetic flux of the stator, θ_{GEN} – the angle between the lines of magnetically inert generator stator

As it was mentioned at the beginning of this chapter, the rotational speed of rotor generator has an attributed rated frequency forming subcarrier frequency ω_N $\{\omega_{N1}, \omega_{N2}, \omega_{N3} \ldots \omega_{Nk}\}$ from certain subassemblies and frequency deviations $\Delta\omega$ $\{\Delta\omega_1, \Delta\omega_2, \Delta\omega_3 \ldots \Delta\omega_k\}$ related with them. Therefore, formula (1) might be developed to the form of:

$$u = k\,B\,\sin[\{\omega_{N1}+\Delta\omega_1, \omega_{N2}+\Delta\omega_2, \omega_{N3}+\Delta\omega_1\}\,t\,p)] \tag{2}$$

Thus, after transformation it looks as follows:

$$u = k\,B\,\sin[\{2\pi f_{N1}+\Delta F_1, 2\pi f_{N2}+\Delta F_2, 2\pi f_{N3}+\Delta F_1\}\,t\,p)] \tag{3}$$

where: f_{N1}, f_{N2}, f_{N3} – subcarrier frequencies of electric waveform, ΔF_1, ΔF_2, ΔF_3 – values of frequency deviation of electric waveform.

Thus, electric waveform of output voltage of generator coupled with turbojet engine reflect, in its frequency modulations, modulations of rotational speed caused by defects of certain mechanical elements, including rolling bearings.

Due to the fact that the number of generator poles is different from the number of rotor grooves, the measurement data is resistant to aliasing effects. Thanks to their characteristics, electric generators transduce the bearing signals within a detection bandwidth substantially higher than other sensors utilized for TTM methods. Each monitored bearing generates a specific fundamental (subcarrier) frequency related to its rotational speed and number of rolling elements [5, 11]. When momentary frequency deviation is plotted against the measured

bearing-specific rotational speed, measurement data-points aggregate around each nominal bearing speed (Fig. 4).

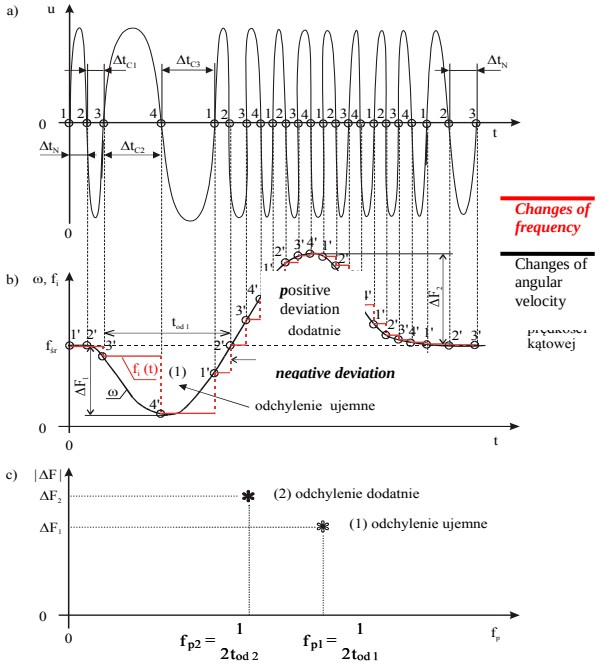

Fig. 3. Formation of characteristic set points: a) instantaneous frequency changes as a function of time – course of the quasi-sinusoidal, b) mapping changes in the frequency plane (ΔF,t_{od})

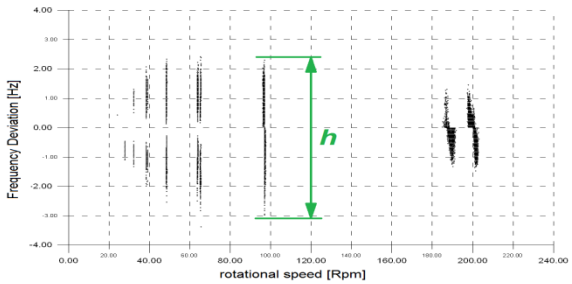

Fig. 4. Visualization of frequency deviation sets, AC generator: *A* - set height parameter

Set height, which is a measure of frequency deviation amplitude, is the main parameter used in signal analysis utilized in the methods. Many of the bearing signal characteristics propagate throughout the system and are picked up by the generator's rotor. The signal output from the generator (which serves as the system's main sensor) is a sum of the bearing spectrum and of the frequency response of the generator itself. High value of generator carrier frequency (order of 100 MHz in the case of DC generators) in comparison to the nominal frequencies of the monitored bearings enables high noise resistance. This modulated signal is not attenuated by the electrical power system of the aircraft, and can be picked up in many points of electrical installation.

3. OPERATIONAL MODELS WEAR OF ROLLING BEARINGS

Author have an extensive experience in monitoring of bearing elements of complex propulsion and transmission systems with the use of FAM-C and FDM-A [7, 9, 16]. Based on these observations, four tribological wear models of the bearing elements were specified. The effects of friction in the bearing itself but also of geometric parameter changes of the engine and accompanying components were taken into account in these models. The wear models of rolling bearing in aircraft engine assembly are as follows: increase of aggregate friction, seizure of rolling elements between races, increase of radial clearance and the related radial resonance phenomenon, increase of axial clearance. These models were devised based on actual data from aircraft system inspection (i.e. bearing supports of the SO-3/3W engines of the TS-11 "Iskra" trainer jet) and presented in the form of symptoms and threshold values applying only to this particular design. The wear models are described in the following chapters. These models portray the representations, of some mechanical wear of rolling bearings of single-shaft turbojet engine in a special way enabling at the same time to observe many occurences inside rolling bearings as well as the location geometry of engine shafts, which were performed thanks to the application of FAM-C and FDM-A methods. Tribological processes are not observed to such extent as changes of spectrum of angular speed. Due to this fact, tribological models also have to be treated as a personal intervention of the author – an attempt to relate extended parameters of characteristic sets to wear condition of rolling bearings of SO-3 engine. Owing to this, it is not a division which stems from tribological theory, but from operational experience. This article does not aim at determining classic tribological models, but only some associations of certain documented wear types of bearings of SO-3 engine along with presentations acquired by the simultaneous (complex) application of FAM-C and FDM-A methods.

4. MODEL OF ROLLING BEARING WITH INCREASED AGGREGATE FRICTION

Increase of friction is a prevalent phenomenon in mechanical bearing operation. It is generally a result of inclusion of foreign objects and rolling surface degradation. An engine wear experiment performed at the Air Force Institute of Technology enabled examination of the general friction increase effects. In the experiment, controlled wearing of the engine middle support bearing was induced in two actual engine test articles [16]. Wear powder – a small grain, silver-steel swarf was continuously introduced into the engines during the experiment. Engine with a higher level of initial internal clearance showcased significant damage already after 3 hours of operation

– wear effects included adhesion of swarf to rolling elements, rise of temperature and plastic deformation, as well as fluctuation of measured tion.

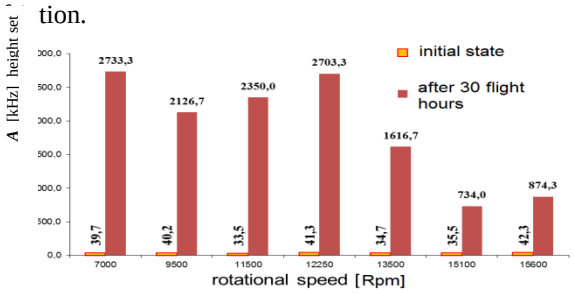

Fig. 5. Increase of set height after 30 hours of operation

Three stages of wearing were observed in the experiment. In the **first stage**, no rolling resistance increase was recorded. In fact, a decrease of frequency deviation set heights was observed by the FAM-C method.

In the **second stage**, an increase of swarf content in the lubricating oil was observed - as well as increase in the measured rolling resistance parameters (i.e. the set height). Locally, a rise in temperature occurred. The surface wear of rolling elements and destruction of oxide and lubricating layers led to some adhesion between bearing elements [8], which changed their model of operation from rolling to sliding (Fig. 7) [11, 18]. In the **third stage**, a decrease of friction forces was observed - a result of local plasticization of the locked rolling elements. Because the surface material layer liquefied due to high temperatures, adhesion between elements stopped and resistance values of rolling bearing something is missing. Some of the rolling elements came to a standstill – stopped to move on races – rolling bearing on this stage became a slide bearing. The operating point moved so the curve Lorenc for a pair of rolling (Fig. 6, curve II) on the curve Lorenc for a pair of sliding (Fig. 6, curve I) resulting from the intensification of consumption per unit of time operation θ [14-15, 18]. For this kind of work, rolling bearings are not structurally designed neither in terms of materials selection, nor in terms of lubrication.

Further wear processes caused by the impurity of lubricating oil with swarf and temperature rise lead to plasticization of the bearing shaft (Fig. 7) and plastic deformation of the bearing support area. This deformation caused changes in engine support geometry and lead to engine unbalance and rapid increase of vibration.

The model of aggregate friction increase is manifested in the FAM-C and FDM-A methods by a diagnostic symptom of the increase of height of characteristic set (for all engine resonance frequencies) [1, 9, 11]. It has been observed that the measured height set increases with service time of the engine. Example of such increase is seen on Fig. 5, where height set increase after 30 flight hours is shown.

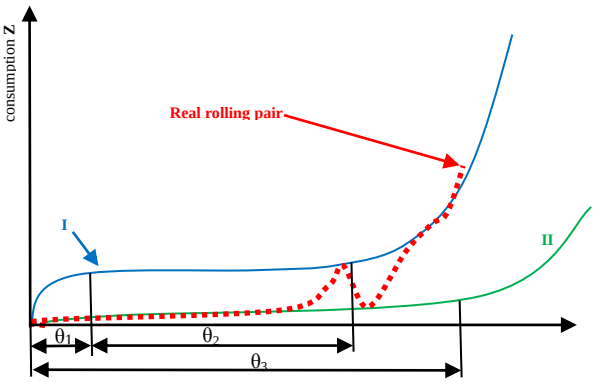

Fig. 6. The Lorenz curie is characterized by wear process of typical working pairs: sliding (I) and rolling (II); θ_1, θ_2 – running-in and consumption period normal for sliding friction, θ_3 – consumption period of the rolling friction till the appearance of the first consumption products as a result of the surface layer fatigue process

Fig. 7. Plasticized bearing journal

Fig. 8. Effect of sliding operation on the bearing rolling elements

5. MODEL OF ROLLING ELEMENT SEIZURE

Seizure of bearing's rolling elements between the bearing races is a wear model that is a result of adhesion forces acting between these components. The adhesion is a result of radial clearance decrease

caused by increased temperature and fluctuations of bearing race compression force [1, 6]. Prolonged operation of a bearing in such state can lead to detrimental effects such as excessive surface wear, pitting corrosion as well as plastic deformation of the rolling elements.

Model of rolling element seizure is manifested in the FAM-C and FDM-A methods by the following diagnostic symptoms [7, 11]:

- height set (DC generator) rises with the nominal engine rotation speed, see Fig. 9;
- for a moderately worn bearing, the rolling coefficient p_s (4) - a measure of the relative rolling rate between the retainer and the races (equation $p_s \approx 1$) increases with engine rotation speed for a critically worn bearing the coefficient monotonically decreases with rotation speed, see Fig. 10:

$$p_S = \frac{f_c}{f_{sh}N} \tag{4}$$

where: f_c – measured set rotational speed, f_{sh} – bearing shaft rotational speed, N - number of rolling elements in the bearing;

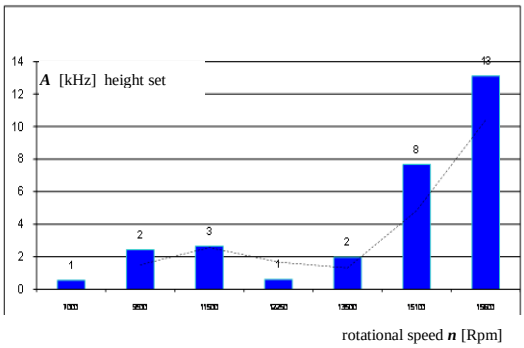

Fig. 9. Model of rolling element seizure (critically worn engine $p_s \approx 0{,}95$) - relationship between engine rotational speed and height set

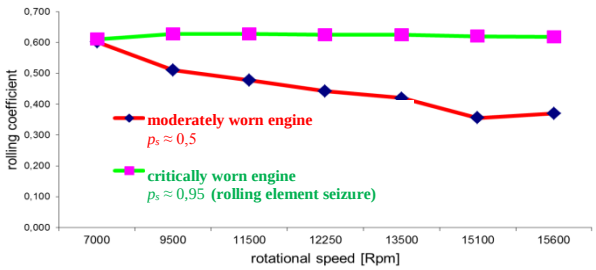

Fig. 10. Model of rolling element seizure – change of rolling coefficient as a function of engine rotational speed

The statistical dispersion of the p_s coefficient increases with engine operation time (for a given engine rotational speed).

According to relationships described by Barwell, on the surfaces of rolling elements and raceways one could find in-tense corrugation with wavelength described with formula (4). Since the radial clearances were too low, the phenomenon affected flexibility of motion of individual rolling elements, in particular, of those of relatively large diameters. The in-crease in friction forces resulted in the heating of rolling-elements' material – fig. 11.

Fig. 10. A rolling element of a bearing with too large interference fit; signs of 'milling' and surface waviness due to heat-induced wear-and-tear are evident

The heating was the greatest in the area of contact with the inner raceway, since it was here where the centrifugal force resulted in the separation of the two surfaces in contact; this, in turn, could provoke longitudinal slip of arcs of both the surfaces in contact, followed with some additional heat-energy release.

6. MODEL OF RADIAL CLEARANCE INCREASE (RESONANSE MODEL)

Increase of bearing radial clearance results in wear effects distinct to the decrease of radial clearance described in the previous wear model. Increased radial clearance may cause dynamic underload of rolling elements [9, 15]. Model of radial clearance increase is manifested in the FAM-C and FDM-A methods by the diagnostic symptoms listed below [1, 9, 11]. For the resonance condition (set Q-factor above 10):

1. height of the DC sets decreases during operation (average height sets falls below 100 Hz) and the sets dissolve into several sub-sets,
2. value of the first harmonic AC frequency increases - result of engine shaft eccentricity increase,
3. the rolling coefficient p_s decreases below nominal value,
4. average bandwidth of the DC sets increases,
5. height set (DC generator) rises with the nominal engine rotation speed ($A = f(n)$), see Fig. 10 shape of 'bath-tube-like' – Fig. 13.

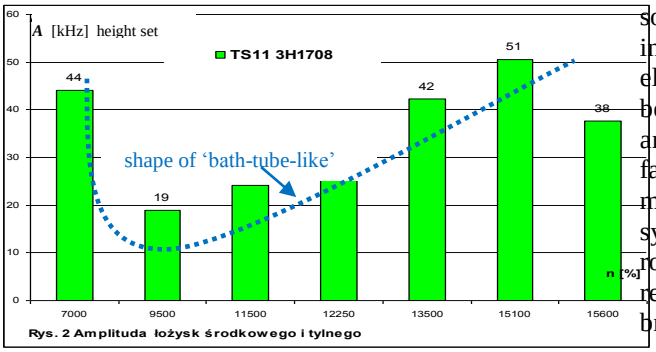

Fig. 11. Model of resonance - relationship between engine rotational speed and height set

Fig. 13 presents an exemplary characteristic set of a resonance-free turbine engine, whereas Fig. 14 shows the same set for a turbine engine with resonance. As the resonant state was approached, the absolute values of heights of the characteristic sets kept decreasing, generally. At the same time, values of true heights kept noticeably increasing. Moderate Q parameters of the sets do not lead to the destruction of the middle engine support bearing of the TS-11 engine even for flight times exceeding 40 h. Also, values of quality factors *Q* of the characteristic sets kept increasing. Following the literature, if the level $Q > 11$ is exceeded, the engine under examination should be withdrawn from service for repair/overhaul. The Authors' engineering practice confirms this relationship.

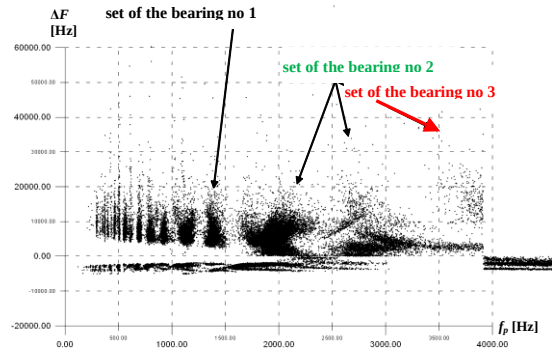

Fig. 13. Characteristic sets for resonance-free bearings

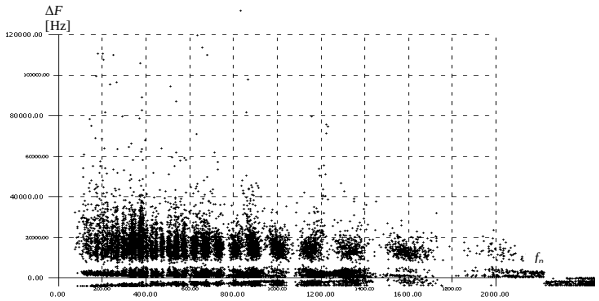

Fig. 14. Characteristic sets for bearings with resonance

The primary conditions conductive to the resonant vibrations during friction are as follows: value of the static friction force higher than that of the force of kinematic friction, and the existence of some elastic bond within the tribological system (i.e. in every sub-system bounded to a friction node's element). The resonant states in the rolling-element bearings may result from many and various factors, among other ones, from enlarged radial clearances, faulty mount of the bearings, or improper storage or maintenance, in particular if in a complete device/ system, e.g. an engine (the neglect to periodically rotate the rotor system). Improper maintenance may result in the origination of the so-called false brinelling (false 'brinell' marks) – fig. 15.

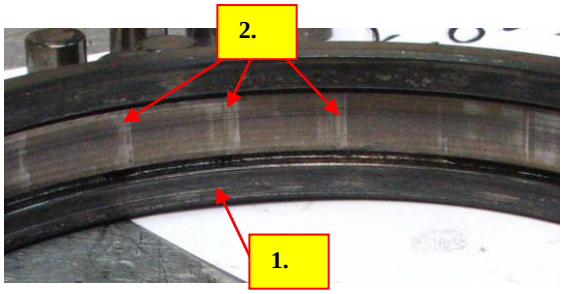

Fig. 15. Components of the bearing of the middle support of a turbine engine: 1 – the outer raceway, 2 – false 'brinell' marks

6. MODEL OF AXIAL CLEARANCE INCREASE

The wear-and-tear induced complex of "excessive axial clearances" is a partially theoretical term invented by the author and reserved for the wear-and-tear phenomena only in the SO-3/3W engines, to be used until sufficiently large amount of data is collected from diagnosing practice with FDM-A and FAM-C methods. This wear-and-tear is featured with particularly complicated dynamics of the 3D motion. While the engine is operating, there is longitudinal (fore-and-aft) motion of both sections of the shaft; also, the actual value of the angle of skew between the two shaft segments keeps changing. Dynamic processes typical for this motion are to a high degree reflected in parameters gained from the alternating current (AC) line, i.e. in the measuring line connected to the output voltage of the rate generator. The plotted curve for the actual frequency $fi = f(t)$ is featured with deep deformations (multiple sharp undercuts/reliefs) in the sinusoidal shape, and modulations of higher frequencies (FM) as well as increased modulations of amplitude (AM) of this time-series plot (Fig. 16). Increase of axial clearance in bearings is a result of relative displacement between portions of the engine shaft, as well as of shaft deformation. This wear model is manifested in the FAM-C and FDM-A methods by the following diagnostic symptoms [8, 11]:

- indents in curve slopes of the AC channel momentary frequency time history are observed,
- height of the first sub-harmonic of AC frequency set is disproportionally large which suggests that large run-outs of compressor shaft in relation to the turbine shaft occurred,

- DC generator sets have disproportionally larger height for mid-range engine rotation speeds, a steady, low frequency oscillatory component can be seen in the signal.

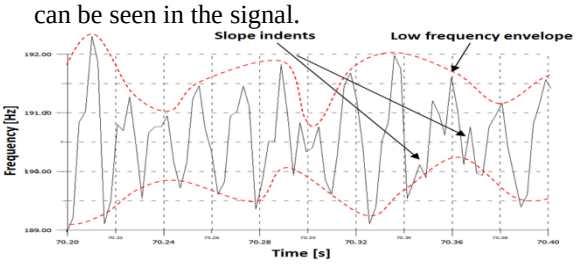

Fig. 16. Example time history, AC generator. Model of axial clearance increase

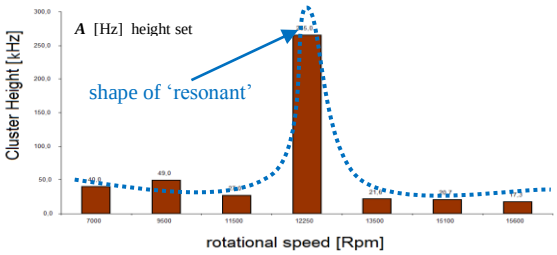

Fig. 17. DC set height vs. engine rotational speed, model of axial clearance increase

With systematised measurements taken with both the FDM-A and the FAM-C methods, having analyses of output signals of on-board generators as the basis, the author have found that there are some dependences between the abovementioned methods and the wear-and-tear processes in the single-shaft turbine engine with "excessive axial clearances" complex. The current state of the engine under examination that shows the wear-and-tear induced complex in question is featured with the following parameters gained with the FDM-A and FAM-C methods [8,11]:

a) on the plot $fi = f(t)$ of the actual AC frequency there are observable deep reliefs (on the rising slope of the quasi-sinusoid) and modulations of higher frequencies (FM) – see Fig. 16; sometimes, single reliefs become multiple – the fast-changing component arises against the quasi-sinusoidal curve of rated frequency of oscillations (that depends on the rated rotational speed of the engine under examination) and a fast-changing component of frequency four times as high (four times as short period of oscillations) appears, value of the relative depth of modulation AM of the $fi = f(t)$ curve for the AC line usually exceeds the 50% level for any rated rotational speed of the engine under examination; after having averaged all the investigated rated rotational speeds of the engine it exceeds the 30% level;

b) the precessional nature (slow descending and then rising of the average value) of the $fi = f(t)$ curve for the AC line (Fig. 16) – the slowly-changing component of the precession takes the oscillatory shape;

c) initially (just after the overhaul/major repair) low values of heights of characteristic sets of the first harmonic of AC of the main shaft's rotational speed systematically increase – values of radial clearances systematically grow;

d) low spans of characteristic sets of the first harmonic of AC of the main shaft's rotational speed – low degree of the ovality of the bearing seating;

f) envelope of curves of heights of characteristic sets for the DC line (of particular bearings) against rated rotational speeds of the engine show shapes that change throughout the whole period of the engine operation:

– the 'resonant' one, i.e. for some rated rotational speed of the engine the increase in heights of sets becomes evident (Fig. 17),
– the 'bath-tube-like';
– the mechanical quality factor Q calculated from the frequency of characteristic sets obtained from the DC line for the middle and rear bearings exceeds 8 (the averaged value for the total of rated rotational speeds of the engine).

7. CONCLUSIONS

In the paper, four wear models of the bearing supports of the SO-3/3W engines of the TS-11 "Iskra" trainer jets were defined as a result of analysis of the tribological process, based on multiple measurements with the use of the FAM-C and FDM-A methods. A set of characteristic diagnostic symptoms can be observed in the analyzed signal for each of the wear models.

The most significant features that describe the wear-and-tear induced complex under examination can also be observed in parameters gained from the DC **(**direct current) line, i.e. in the measuring line connected to DC generator's output voltage. Envelope of heights of characteristic sets for the DC line (of particular bearings) against rated rotational speeds of the engine for different wear-and-tear induced complexes take different shapes:

– exponentially descending - for the bearing that shows ideal performance,
– 'bath-tube-like' - for the resonant condition of the bearing support,
– rising - for the bearings with too large interference fits, with increased rolling resistance (friction),
– 'resonant', i.e. with increased height of characteristic sets for one rated frequency in case there is excessive total resistance/friction.

Diagnostic experience suggests that these symptoms reliably indicate the wear level of the analyzed engine. However, the presented method has to be calibrated for any new engine model or transmission system, as the bearing wear models presented here only apply to the SO-3/3W design. Other design may have distinct sets of diagnostic symptoms and signal threshold levels. Currently, interpretation of

the FAM-C and FDM-A results relies on the experience of the analyst. A more formal automated method of result analysis is being developed by the author.

BIBLIOGRAPHY

1. Barwell FT. Lubrication of bearings. 1956.
2. Bilinkis I. Digital Alias-free Signal Processing. ISBN 978-0-470-02738-7.
3. Campbell W.: Elastic fluid turbine rotor and method of avoiding tangential bucket vibration threin. Patent US 1.502.904.
4. Carrington IB, Wright JR, Cooper JE, Dimitriadis G. A comparison of blade tip timing data analysis methods. Proceedings of the Institution of Mechanical Engineers, Part G, Journal of Aerospace Engineering, 2001; 215(5): 301-312.
5. Chuan Li, Vinicio Sanchez, Grover Zurita, Mariela Cerrada Lozada, Diego Cabrera: Rolling element bearing defect detection using the generalized synchrosqueezing transform guided by time-frequency ridge enhancement, ISA Transactions, 2016; 60: 274-284.
6. Ma GJ, Wu CW, Zhou P. Influence of Wall Slip on the Dynamic Properties of a Rotor-Bearing System. Tribology Transactions, 2008; 51: 204-212.
7. Gębura A, Tokarski T. Metody FDM-A i FAM-C w wykrywaniu i monitorowaniu silnie zaciśniętych łożysk tocznych, Prace Naukowe Instytutu Technicznego Wojsk Lotniczych, 2008; 23: 223-235
8. Gębura A, Tokarski T. The monitoring of the Bearing joints with excessive axial clearances using the FAM-C and FDM-A methods, Research Works of Air Force Institute of Technology (Prace Naukowe ITWL), 2010; 27: 105-137.
9. Gębura A, Tokarski T. The monitoring of the Bearing nodes with excessive radial clearances using the FAM-C and FDM-A methods, Research Works of Air Force Institute of Technology (Prace Naukowe ITWL), 2009; 25: 89-127.
10. Gębura A, Pietnoczko B, Tokarski T. Diagnostic testers operating on the basis of the FAM-C method. Diagnostyka, 2016; 17(3): 87-94.
11. Gębura A. Inspecting the technical condition of bearing assemblies and selected elements of power unit transmission, 2014, Warsaw: Publisher of the Air Force Institute of Technology.
12. Hermans L, Van der Auweraer H. Modal Testing and Analysis of Structures under Operational Conditions. Mechanical System and Signal Processing, 1990: 1(2):193-216.
13. Sawalhi N, Randall R. Effects of limiting the bandwidth of the vibration signal on bearing fault detection and diagnosis using state of the art techniques, AIAC-13 Thirteenth American International Aerospace Congress; Sixth DSTO, 2013.
14. Skoć A, Spałek J, Makusik S. Podstawy konstrukcji maszyn, T. 2, Wydawnictwo Naukowo-Techniczne, Warszawa 2008.
15. Spałek J. Problemy inżynierii smarowania maszyn w górnictwie, Wydawnictwo Politechniki Śląskiej, Gliwice 2003.
16. Spychała P, Majewski P, Szczekala M, Gębura A. Badania silnika 308 w hamowni WZL-3, Warszawa 2006.
17. Sung-HoonJeng, Seok-Ju Yong. Friction and wear characteristic Due to stick-slip under fretting condition, Tribology Transactions, 2004; 50:564-722.
18. Szurgacz D. Tribological aspects of machine operation in mining engineering. Research Reports of Central Mining Institute. Mining & Environment, 2010; 1.
19. Wang W. Damage Detection of Gas Turbine Engine By Analyzing Blade Tip Timing Data. Proc. Of HUMS 2003. Conference, DSTO, Australia.
20. Witoś M. Increasing the durability of turbine engines through active diagnostics and control`. Research Works, 2011; 29.
21. Woch M, Matyjewski M, Kurdelski M. Reliability at the checkpoints of an aircraft supporting structure, Maintenance and Reliability,2015; 17(3):457-462.
22. Woch M, Nowakowski T, Młynarczyk M. Conference „Proceeding of the European safety and Reliability Conference (CSREL), location Wrocław Metodology and Applications, 2015:2355-2360.
23. Żurek J, Tomaszek H, Zieja M. Analysis of structural component's life time distribution considered from the aspect of the wearing with the characteristic function applied, 22nd Annual Conference on European Safetly and Reliability (ESREL), SEP 29-OCT 02.2013, Amsterdam "Safety Reliability and Risk Analysis: Beyond the Horizon", 2013: 2597-2602.

Received 2016-12-20
Accepted 2017-02-24
Available online 2017-03-23

dr inż. **Andrzej GĘBURA** – absolwent Wojskowej Akademii Technicznej na kierunku elektromechanika specjalność osprzęt lotniczy, w latach 1973-1978. 1998 obronił rozprawę doktorską w Instytucie Technicznym Wojsk Lotniczych, Autor 106 publikacji w tym 2 monografii naukowych. Prowadzi prace w zakresie elektroenergetyki lotniczej oraz diagnostyki mechanicznych zespołów napędowych metodami elektrycznymi.